Rough Surface Contact

T Nguyen, B Alzahabi*
Kettering University, USA

ABSTRACT
This paper studies the contact of general rough curved surfaces having nearly identical geometries, assuming the contact at each differential area obeys the model proposed by Greenwood and Williamson. In order to account for the most general gross geometry, principles of differential geometry of surface are applied. This method while requires more rigorous mathematical manipulations, the fact that it preserves the original surface geometries thus makes the modeling procedure much more intuitive. For subsequent use, differential geometry of axis-symmetric surface is considered instead of general surface (although this "general case" can be done as well) in Chapter 3.1. The final formulas for contact area, load, and frictional torque are derived in Chapter 3.2.

1. INTRODUCTION
The need of understanding rough surfaces contact has long been recognized. One primary focuses of the early studies is to predict real contact area as it varies with load. Since a rough surface is known to include layers of micro-asperities, the real area of contact can be extremely small comparing to the apparent area observed by our eyes and is very difficult to measure. This problem has been addressed and resolved for the first time by Archard, Greenwood and Williamson using novel fractal and statistical models to mathematically describe the microscopic surface structure. Their works have been the basis for various subsequent studies on contact mechanics, describing the surface geometry (asperities distribution, geometry) and material behavior (elastic, plastic flow) (Yastrebov et al. 2014). Recently, a deterministic approach to model rough surface contact has grown rapidly with the advance of computational capability, providing further insights to the study of contact mechanics.

The fact that only nominally flat rough surfaces case is focused has limited the scope of this model. One reason for this shortage was given by Greenwood and Trip, as generally the curvatures difference of curved surfaces creates a cluster effect which makes asperities interaction becomes significant. Thus an intensive analysis similar to those performed in the nominally flat rough surfaces contact is not frequently performed in the case of rough curved surfaces contact. Rather, the latter in only loosely studied through the inspection of axial contact between two rough curved surfaces having constant curvatures, by replacing them with a nominally flat rough surface and a smooth curved surface having anequivalent-curvature (Johnson 1985). This method although gives a quick approximation of pressure distribution, it does not allow one to account for:

- More general analysis, such as the contact is non-axial or the surfaces have varying curvatures

*Corresponding Author: balzahab@kettering.edu

- More detailed analysis, such as the true distribution of contact pressure which is important to the calculation of cumulative frictional torque in rotating parts.

This paper studies the contact of general rough curved surfaces having nearly identical geometries, assuming that the contact at each differential area obeys the model proposed by Greenwood and Williamson (GW model for short). In order to account for the most general geometry, principles of differential geometry of surface are applied. This method requires more rigorous mathematical manipulations, as it preserves the original surface geometries (i.e. not require the original system to be replaced by any equivalent system) makes the modeling procedure much more intuitive. For subsequent use, differential geometry of axis-symmetric surface is considered instead of general surface (although this "general case" can be done as well) in Chapter 3.1. The final formulas for contact area, load, and frictional torque are derived.

One direct application of this study is the analysis of roughness-dependent frictional torque occuring rotating parts, whose geometry is often axis-symmetric. For flat surfaces contact (i.e. two flat surfaces slide across each other), effect of friction is generally quantified with the calculation of frictional force value. Similarly, for curved surface contact (e.g. in journal bearing), the value of frictional torque is frequently required. Unlike the former situation, where surface roughness does not affect the frictional force if one uses the Coulomb's friction model (since the total reaction force at the points of asperity contact always equal to the load), surface roughness changes the distribution of contact pressure across the curved surfaces (even when Coulomb's model holds), thus frictional torque value would be different. Furthermore, the frictional torque will not vary linearly with the load like when one models contacting surfaces smooth, rather it will also be dependent on the roughness. This topic is clarified through two specific examples. Lastly, additional analysis on the load – contact area and frictional torque – load relationship is presented.

2. MODELING ROUGH SURFACE CONTACT:

Greenwood and Williamson (1966) proposed a method to mathematically model the stochastic nature of surface's microscopic structure by using a probabilistic approach, which introduce the concept of "asperity" and consider their height to be normally distributed over the entire rough surface. In practice, such statement is valid for most high-end engineering surfaces (i.e. homogeneous, isotropic surface), yet not quite so for other lower-end ones (Bhushan 2001). For the latter situation, Kotwal and Bhushan (1996) have developed an analytical method to generate probability density functions of non-Gaussian distributions, but will not be considered in this study. One key assumption in the work of Greenwood and Williamson is that each individual contact does not affect the deformation of its neighbors and the asperity is spherical with curvature $\Re_0$ at its peak (Figure 1). This conveniently allows the each individual contact to be modeled independently by implementing the Hertzian theory. As mentioned previously, this method limits the contact to only be between nominally flat rough surfaces, so that the above assumption holds.

Consider two rough surfaces in contact which could be replaced by a system of two other surfaces with equivalent asperities' curvature and RMS roughness parameter. The first surface is perfectly smooth and is located at some distance l_0 from the reference line h_0. The second surface is considered rough with the asperities' height z varies randomly around the reference line which is described by the Gaussian distribution (Skewness = 0 and Kurtosis = 3) (Figure 2):

$$\Phi(z) = \frac{1}{\sqrt{2\pi}R_q} \exp\left(-\frac{(z-h_0)^2}{2R_q^2}\right) \tag{1}$$

where R_q is the RMS roughness parameter.

If the total number of asperities on this surface is N_0, the number of asperities having height in the interval $[z, z+dz]$ comes into contact is $\nu = N_0\Phi(z)dz$ and thus the total number of asperities in contact is $N = \int_{x_1}^{x_2}\int_{l_0}^{\infty} \nu = \int_{x_1}^{x_2}\int_{l_0}^{\infty} N_0\Phi(z)dz$.

Furthermore, according to the Hertzian contact theory, when a elastic sphere is indented to depth $z-l_0$ (from now refer as the indentation depth) in an elastic half-space:

The contact area is $A_{\sin g} = \pi a^2 = \pi\Re_0(z-l_0)$ and the required force is $F_{\sin g} = \frac{4}{3}E^*\Re_o^{1/2}(z-l_0)^{3/2}$.

Thus the cumulative contact area is $A = \int_{x_1}^{x_2}\int_{l_0}^{\infty} \nu A_{\sin g} = \int_{x_1}^{x_2}\int_{l_0}^{\infty} \pi\Re_0(z-l_0)\times N_0\Phi(z)dz$ and the cumulative required force is $F = \int_{x_1}^{x_2}\int_{l_0}^{\infty} \nu F_{\sin g} = \int_{x_1}^{x_2}\int_{l_0}^{\infty} \frac{4}{3}E^*\Re_o^{1/2}(z-l_0)^{3/2}\times N_0\Phi(z)dz$ with E^* is the equivalent modulus of elasticity and can be found using $\frac{1}{E^*} = \frac{1-\nu_1^2}{E_1} + \frac{1-\nu_2^2}{E_2}$ (E_1, E_2, ν_1, ν_2 are the moduli of elasticity and Poisson's ratios of the two bodies) (Figure 3).

Noting that if a thin layer of coating is present, according to Liu et al (2005) a different equivalent modulus of elasticity should be used.

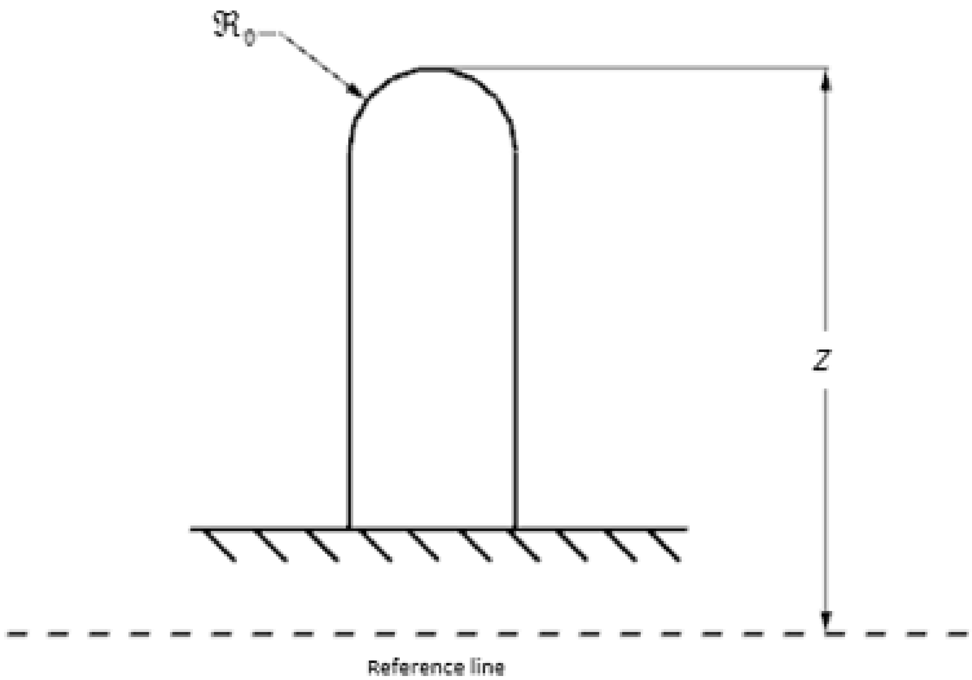

Figure 1. GW model of a single asperity

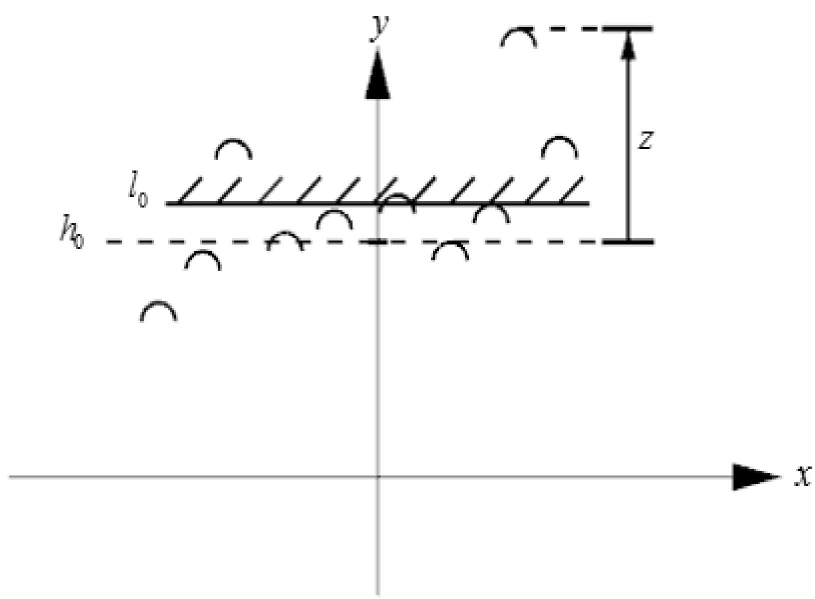

Figure 2. GW model of rough surfaces contact

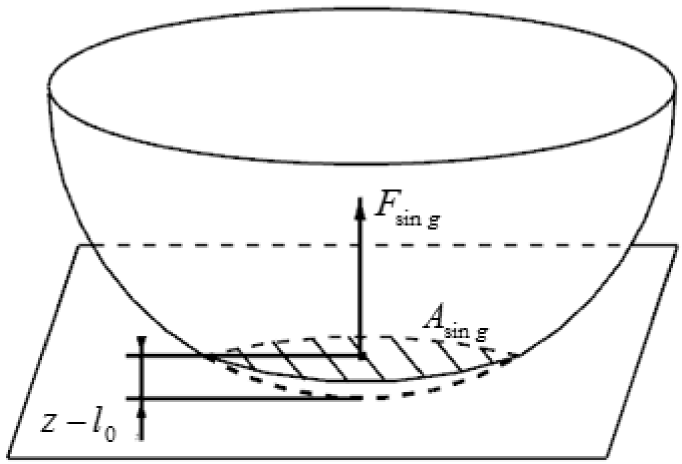

Figure 3.Contact between a elastic sphere and elastic half-space

Very recently, the exact solutions for these integrals have been found in Jackson and Green (2011):

If $I_{ep} = \int_a^\infty (z-a)^{3/2}\Phi(z)dz \;\; with \;\; \Phi(z) = \frac{1}{\sqrt{2\pi}}\left(\frac{1}{\sigma_s}\right)\exp\left(\frac{z^2}{2\sigma_s^2}\right)$ and $I_{ea} = \int_a^\infty (z-a)\,\Phi(z)dz$, then:

$$I_{ep} = \begin{cases} \frac{1}{4\sqrt{\pi}}\left(\frac{1}{\sigma_s}\right)\sqrt{a}\exp(-\gamma)\left[(1+\alpha^2)K_{1/4}(\gamma) - \alpha^2 K_{3/4}(\gamma)\right] \text{-----------------} a > 0 \\ \frac{1}{2^{1/4}\sqrt{\pi}}\Gamma\left(\frac{5}{4}\right)\left(\frac{1}{\sigma_s}\right)^{3/2} \text{--------------------------------} a = 0 \\ \frac{1}{4}\sqrt{\frac{\pi}{2}}\left(\frac{1}{\sigma_s}\right)\sqrt{-a}\exp(-\gamma)\left[(1+\alpha^2)I_{-1/4}(\gamma) + (3+\alpha^2)I_{1/4}(\gamma) + \alpha^2(I_{3/4}(\gamma) + I_{5/4}(\gamma))\right] \text{---} a < 0 \end{cases} \tag{2}$$

$$I_{ea} = \sqrt{\frac{1}{2\pi}}\left(\frac{1}{\sigma_s}\right)\exp(\frac{-\alpha^2}{2}) - \frac{a}{2} erfc\left(\frac{\alpha}{\sqrt{2}}\right) \tag{3}$$

where:

$\alpha = \frac{a}{\sigma_s}, \gamma = \frac{\alpha^2}{4}$

$I(\cdot)$ and $K(\cdot)$ are the modified Bessel function of the first & second kind respectively

$erfc(\cdot)$ is the complimentary error function

$\Gamma(\cdot)$ is the gamma function

3. NEARLY-IDENTICAL ROUGH CURVED SURFACES CONTACT:

Since the two curved surfaces considered in this study are nearly-identical, contact at each infinitesimal area could be treated as the contact between two nominally flat rough surface, which can then be integrated to describe the overall contact behavior between gross geometries. This approach requires the number of asperities and the indentation depth at each differential surface contact to be found. Furthermore, the magnitude, direction and location of application of contact pressure (i.e. define a bound vector) at each individual asperity as well as corresponding differential surface area should also be stated. What is known is the applied load, geometry and material properties of considered surfaces, and therefore any expression should be written in terms of these given parameters.

3.1. Differential geometry of surfaces:

i) Vector formalism of line in 3D space:

It is very convenient to express a general bound vector in 3D space using vector formulation. A bound vector is completely defined if its initial point, magnitude and direction are specified. In this problem, three quantities need to be expressed vectorially are the asperity's direction, the reaction force and the friction force.

Consider a straight line L is defined by two parameters $(\underline{x}_P, \overline{\ell})$ (Figure 4). An arbitrary point Q on the line has position vector $\underline{x}_Q$ is given by $\underline{x}_Q = \underline{x}_p + \lambda\overline{\ell}$ where λ is an arbitrary scalar.

We are also interested in he point where an asperity comes into contact: a point I is the intersection of two line $L1 = (\underline{x}_1, \overline{\ell_1})$ and $L2 = (\underline{x}_2, \overline{\ell_2})$ has position vector $\underline{x}_I$ given by:

$$\underline{x}_I = \underline{x}_1 + \lambda_1\overline{\ell_1} = \underline{x}_2 + \lambda_2\overline{\ell_2} \tag{4}$$

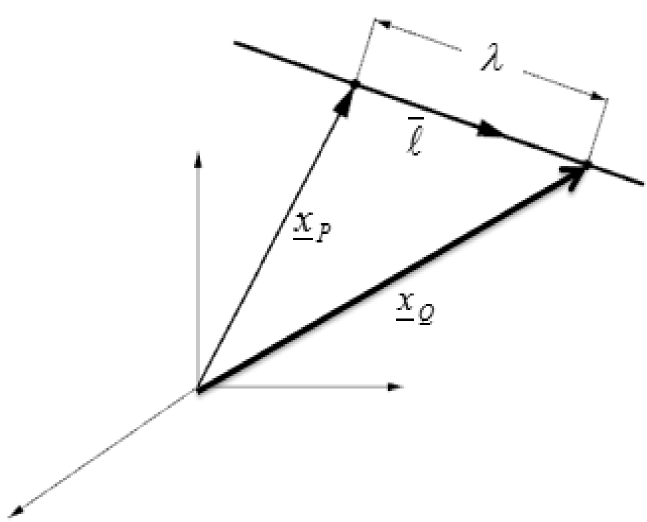

Figure 4. 3D line parameters

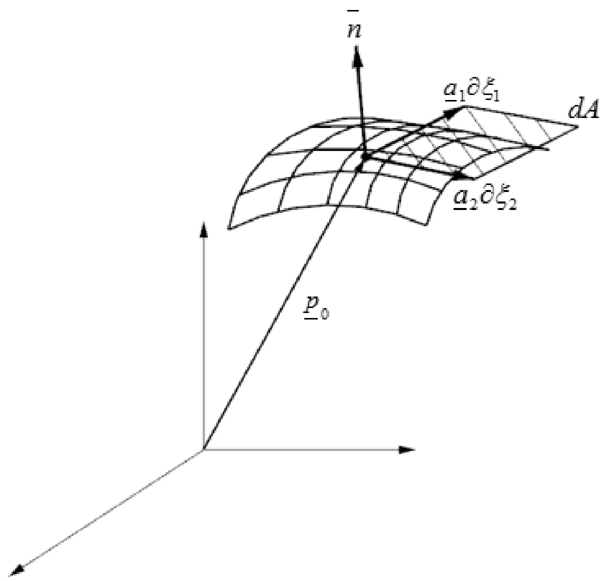

Figure 5. 3D surface parameters

ii) Differential geometry of surface of revolution:

To understand the contact of any asperity on the surface, differential geometry is used to describe many of the surface's characteristics as function of surface's parameters (Figure 5).

A general surface S in 3D space can be generated by two parameters ξ_1 and ξ_2. Any point on the surface has the position vector $\underline{p} = \underline{p}(\xi_1, \xi_2)$. In orthonormal coordinates the surface of revolution can always be expressed as (Gray 1997):

$$\underline{p}(\xi_1, \xi_2) = \begin{Bmatrix} \phi(\xi_2)\cos(\xi_1) \\ \phi(\xi_2)\sin(\xi_1) \\ \psi(\xi_2) \end{Bmatrix} \tag{5}$$

Let $\dfrac{\partial \underline{p}_0}{\partial \xi_1} = \underline{a}_1$ and $\dfrac{\partial \underline{p}_0}{\partial \xi_2} = \underline{a}_2$:

$$\underline{a}_1 = \left[-\varphi\sin(\xi_1) \quad \varphi\cos(\xi_1)\right]^T$$

$$\underline{a}_2 = \left[-\varphi'\cos(\xi_1) \quad \varphi'\sin(\xi_1) \quad \psi'\right]^T$$

$$\underline{a}_1 \times \underline{a}_2 = \left[\varphi(\psi'\cos(\xi_1) \quad \varphi\psi'\sin(\xi_1) \quad -\varphi\varphi'\right]^T$$

$$\left\|\underline{a}_1 \times \underline{a}_2\right\| = |\varphi|\sqrt{\psi'^2 + \varphi'^2}$$

The unit normal vector $\bar{n}$ of the surface is:

$$\bar{n}(\xi_1,\xi_2) = \frac{\tilde{a}_1 \underline{a}_2}{\|\tilde{a}_1 \underline{a}_2\|} = \frac{\operatorname{sgn}(\phi)}{\sqrt{\phi'^2 + \psi'^2}} \begin{Bmatrix} \psi' \cos(\xi_1) \\ \psi' \sin(\xi_1) \\ -\phi' \end{Bmatrix} \tag{6}$$

$$dA = \|\tilde{a}_1 \underline{a}_2\| \, d\xi_1 d\xi_2 = \operatorname{sgn}(\phi)\phi\sqrt{\psi'^2 + \phi'^2} \, d\xi_1 d\xi_2 \tag{7}$$

For a surface of revolution, it is natural to pick $\xi_1 = r$, $\xi_2 = \phi$ (Figure 6).

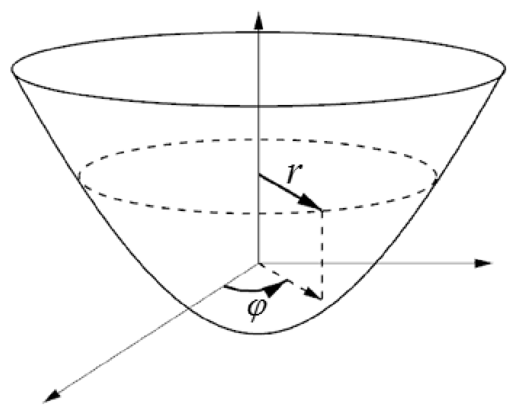

Figure 6. A general surface of revolution

If a surface is obtained by rotating the curve $z = f(r)$ from $z = z_1$ to $z = z_2$ around the $z - axis$, from Eq. (5) any point on this surface has the position vector:

$$\underline{p}(r,\varphi) = \begin{Bmatrix} r\cos\varphi \\ r\sin\varphi \\ f(r) \end{Bmatrix} \tag{8}$$

with $\varphi(r) = r$ and $\psi(r) = f(r) = z$.

From Eq. (6) and Eq. (7) , the corresponding unit normal vector $\bar{n}$ and the corresponding area of a differential surface element dA is:

$$\bar{n}(r,\varphi) = \frac{1}{\sqrt{1+(z')^2}} \begin{Bmatrix} z'\cos(\varphi) \\ z'\sin(\varphi) \\ 1 \end{Bmatrix} \tag{9}$$

$$dA = \sqrt{1+(z')^2}\; rdrd\varphi \tag{10}$$

Furthermore, if $g(z) = f^{-1}$, the (apparent) area of this surface given by Anton (1999) is:

$$A_{apperent} = 2\pi \int_{z_1}^{z_2} g(z)\sqrt{1+[g'(z)]^2}\,dz \tag{11}$$

3.2. Calculation of contact area, contact pressure and frictional torque:

Consider a surface of revolution S1 with vertex O_1 is at the origin of frame $\Re_1 = (\overline{i_1}, \overline{i_2}, \overline{i_3})$ and a surface of revolution S2 with vertex O_2 is at the origin of frame $\Re_2 = (\overline{j_1}, \overline{j_2}, \overline{j_3})$ (Figure 7). $(\overline{i_1}, \overline{i_2}, \overline{i_3})$ can always be chosen such that the position vector of O_2 with respect to $\Re_1$ is the eccentricity vector $\underline{e} = \begin{bmatrix} e_x & 0 & e_z \end{bmatrix}^T$. Because the surface is axis-symmetric and the asperities are randomly distributed, the eccentricity vector is assumed to be parallel to the load $\underline{F} = \begin{bmatrix} F_r & 0 & F_z \end{bmatrix}^T$, which is a known vector.

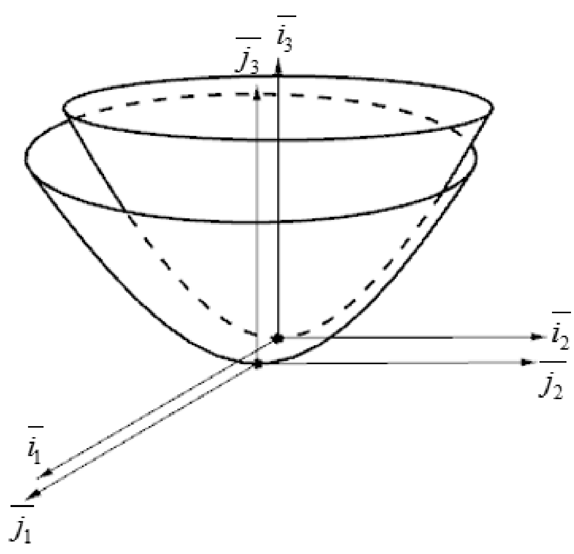

Figure 7. Contacting surfaces of revolution

According to the GW model, let S1 is a rough surface and S2 is a perfectly smooth surface. The geometries of S1 and S2 are generated by rotating the curves $z_1 = f_1(r_1)$ and $z_2 = f_2(r_2)$ around $\overline{i_3}$ *and* $\overline{j_3}$ respectively.

Consider a differential area at point I_1 on the rough surface S1 defined by two parameters (r_1, ϕ_1) and associated with the normal vector $\overline{n_1}(r_1, \phi_1)$ (resolved in $\Re_1$). $\overline{n_1}$ intersects the smooth surface S2 at point I_2. $\overline{n_2}(r_2, \phi_2)$ is normal vector of the smooth surface S2 at point I_2 (resolved in $\Re_2$). From Eq. (9) and Eq. (10):

$$\overline{n_1} = \begin{bmatrix} \dfrac{z_1' \cos(\varphi_1)}{\sqrt{1+(z_1')^2}} & \dfrac{z_1' \sin(\varphi_1)}{\sqrt{1+(z_1')^2}} & \dfrac{1}{\sqrt{1+(z_1')^2}} \end{bmatrix}^T = \begin{bmatrix} n_{1,x} & n_{1,y} & n_{1,z} \end{bmatrix}^T \tag{12}$$

$$\overline{n_2} = \begin{bmatrix} \dfrac{z_2' \cos(\varphi_2)}{\sqrt{1+(z_2')^2}} & \dfrac{z_2' \sin(\varphi_2)}{\sqrt{1+(z_2')^2}} & \dfrac{1}{\sqrt{1+(z_2')^2}} \end{bmatrix}^T = \begin{bmatrix} n_{2,x} & n_{2,y} & n_{2,z} \end{bmatrix}^T \tag{13}$$

$$dA = \sqrt{1+(z_1')^2}\, r_1 dr_1 d\varphi_1 \tag{14}$$

Introduce $\Delta(r_1, \phi_1) = d(I_1, I_2)$ and $\delta = d(I_1, P)$ with P is any point on the line $I_1 I_2$. Physically, δ, $\overline{n_1}$, $\overline{n_2}$ represent the height, the direction of an individual asperity and the direction of reaction force respectively (Figure 8).

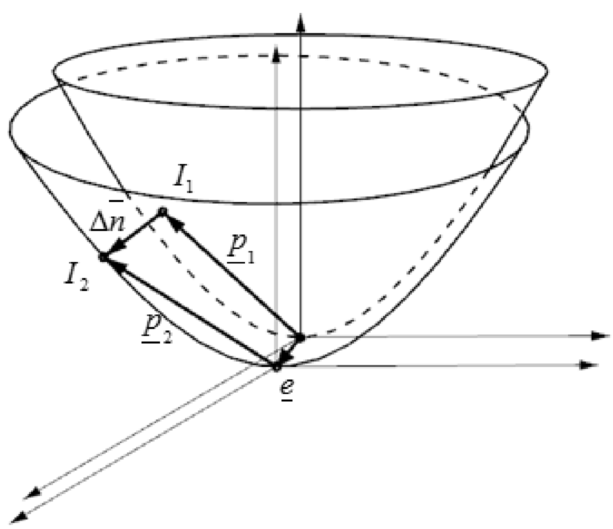

Figure 8. Representation of several surface parameters

System of equations for the intersection at I_2 can then be derived from Eq. (4) and Eq. (8):

$$\begin{Bmatrix} e_x + r_2\cos(\varphi_2) \\ r_2\sin(\varphi_2) \\ e_z + z_2 \end{Bmatrix} = \begin{Bmatrix} \Delta(r_1,\varphi_1)n_{1,x} + r_1\cos(\varphi_1) \\ \Delta(r_1,\varphi_1)n_{1,y} + r_1\sin(\varphi_1) \\ \Delta(r_1,\varphi_1)n_{1,z} + z_1 \end{Bmatrix} \tag{15}$$

By solving this system, we obtain $\Delta(r_1,\phi_1)$ as well as $r_2(r_1,\phi_1)$, $\phi_2(r_1,\phi_1)$. Substitute $r_2(r_1,\phi_1)$, $\phi_2(r_1,\phi_1)$ into Eq. (13), we could express $\overline{n_2}$ in terms of r_1 and ϕ_1. The indentation depth of an individual asperity can be found as:

$$\Im(r_1,\varphi_1) = \Re_0 - (\Delta + \Re_0 - \delta)\cos(\theta) \tag{16}$$

with $\cos(\theta) = \overline{n_1}^T \overline{n_2}$ (Figure 9).

In a differential area, the asperities can be assumed to be unidirectional (i.e. having the same direction vector). If the asperities density is $\aleph_0$, The number of asperities in that differential area is $\aleph_0 dA = \aleph_0\sqrt{1+(z_1')^2}\, r_1 dr_1 d\phi_1$. Since the asperities' height is normally distributed described by the Gaussian distribution, the number of asperities on a differential area that height in the interval $[\delta, \delta + d\delta]$ is:

$$\nu = \aleph_0 dA \times \Phi(\delta)d\delta = \aleph_0\Phi(\delta)\sqrt{1+(z_1')^2}\, r_1 dr_1 d\varphi_1 d\delta \tag{17}$$

In terms of contact pressure distribution:

$$\underline{\Pi} = \frac{\nu \times \underline{F}}{dA} = \int_{\Delta}^{\infty} \frac{4}{3} E^* \Re_o^{1/2} \aleph_0 \Phi(\delta) \Im^{3/2} d\delta \times \overline{n_2}$$

In terms of contact pressure distribution:

$$\underline{\Pi} = \frac{\nu \times \underline{F}}{dA} = \int_{\Delta}^{\infty} \frac{4}{3} E^* \Re_o^{1/2} \aleph_0 \Phi(\delta) \Im^{3/2} d\delta \times \overline{n_2}$$

Furthermore, the position vector of a single point of contact I_1 and the moment arm (Figure 10) respectively are:

$$\underline{p}_{\sin g} = \underline{p}_1 + \Delta(r_1, \varphi_1)\overline{n_1}$$

$$\underline{p'}_{\sin g} = \underline{p}_{\sin g} - (\underline{p}^T_{\sin g}\, \overline{i_3})\overline{i_3} \tag{18}$$

Assume the relative angular velocity is $\varpi \overline{i_3}$, the directional unit vector of the frictional force at an asperity contact is:

$$\overline{n_f} = \left[\frac{\mathrm{sgn}(\varpi)\,\mathrm{sgn}(n_{2,x})n_{2,y}}{\sqrt{n_{2,x}^2 + n_{2,y}^2}} \quad \frac{-\,\mathrm{sgn}(\varpi)\,\mathrm{sgn}(n_{2,x})n_{2,x}}{\sqrt{n_{2,x}^2 + n_{2,y}^2}} \quad 0 \right]^T \qquad (\overline{n_f}^T\, \overline{n_2} = 0) \tag{19}$$

Finally, we attain the expressions for the number of asperities, real contact area, reaction force components and frictional torque in terms of an individual asperity, a differential surface area and the entire contacting surfaces:

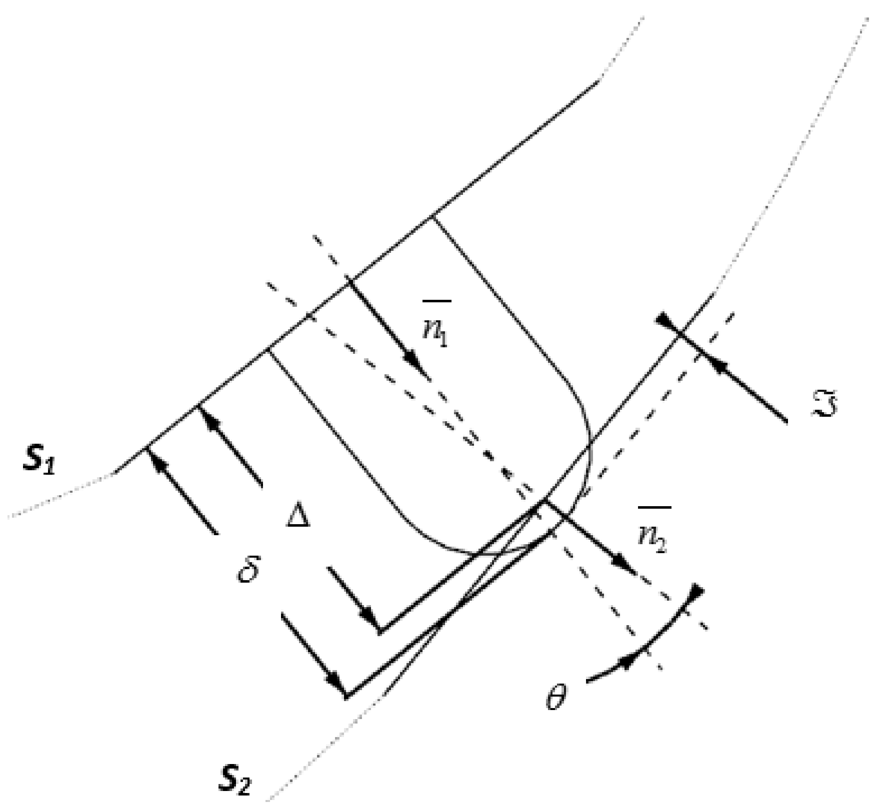

Figure 9. Contact of a single asperity

Table 1. Expressions for the number of asperities, real contact area, reaction force components and frictional torque

Number of asperities in contact	Single asperity	1
	Differential surface area	$\nu = \aleph_0 \Phi(\delta)\sqrt{1+(z_1')^2}\; r_1 dr_1 d\varphi_1 d\delta$
	Entire surface	$\int_o^{2\pi}\int_d^{dz}\int_\Delta^{\infty} \nu = N_c \quad (20)$
Real contact area	Single asperity	$A_{\sin g} = \pi \Re_0 \Im$
	Differential surface area	$A_{diff} = \nu \times A_{\sin g} = \pi \Re_0 \aleph_0 \Phi(\delta) \Im \sqrt{1+(z_1')^2}\; r_1 dr_1 d\varphi_1 d\delta$
	Entire surface	$\int_o^{2\pi}\int_d^{dz}\int_\Delta^{\infty} A_{diff} = A_{real} \quad (21)$
Reaction force (x - component)	Single asperity	$F_{\sin g,x} = \frac{4}{3} E^* \Re_o^{1/2} \Im^{3/2} \times (\overline{n_2}^T \, \overline{i_1})$
	Differential surface area	$F_{diff,x} = \frac{4}{3} E^* \Re_o^{1/2} \aleph_0 \Phi(\delta) \Im^{3/2} \sqrt{1+(z_1')^2}\; r_1 dr_1 d\varphi_1 d\delta \times (\overline{n_2}^T \, \overline{i_1})$
	Entire surface	$\int_o^{2\pi}\int_d^{dz}\int_\Delta^{\infty} F_{diff,x} = F_x \quad (22)$
Reaction force (y - component)	Single asperity	$F_{\sin g,y} = \frac{4}{3} E^* \Re_o^{1/2} \Im^{3/2} \times (\overline{n_2}^T \, \overline{i_2})$
	Differential surface area	$F_{diff,y} = \frac{4}{3} E^* \Re_o^{1/2} \aleph_0 \Phi(\delta) \Im^{3/2} \sqrt{1+(z_1')^2}\; r_1 dr_1 d\varphi_1 d\delta \times (\overline{n_2}^T \, \overline{i_2})$
	Entire surface	$\int_o^{2\pi}\int_d^{dz}\int_\Delta^{\infty} F_{diff,y} = 0 \quad (23)$
Reaction force (z - component)	Single asperity	$F_{\sin g,z} = \frac{4}{3} E^* \Re_o^{1/2} \Im^{3/2} \times (\overline{n_2}^T \, \overline{i_3})$
	Differential surface area	$F_{diff,z} = \frac{4}{3} E^* \Re_o^{1/2} \aleph_0 \Phi(\delta) \Im^{3/2} \sqrt{1+(z_1')^2}\; r_1 dr_1 d\varphi_1 d\delta \times (\overline{n_2}^T \, \overline{i_3})$
	Entire surface	$\int_o^{2\pi}\int_d^{dz}\int_\Delta^{\infty} F_{diff,z} = F_z \quad (24)$
Frictional torque	Single asperity	$\underline{T}_{\sin g} = \frac{4}{3} \mu E^* \Re_o^{1/2} \Im^{3/2} \times (\tilde{p}_{\sin g} \overline{n_2})$
	Differential surface area	$\underline{T}_{diff} = \nu \times \underline{T}_{\sin g} = \frac{4}{3} \mu E^* \Re_o^{1/2} \aleph_0 \Phi(\delta) \Im^{3/2} \sqrt{1+(z_1')^2}\; r_1 dr_1 d\varphi_1 d\delta \times (\tilde{p}'_{\sin g} \overline{n_f})$
	Entire surface	$\int_o^{2\pi}\int_d^{dz}\int_\Delta^{\infty} \underline{T}_{diff} = \underline{T}_f \quad (25)$

Eq. (20) shows the number N_c of asperities that are in contact. Eq. (21) can be solved using Eq. (3) that approximates the real contact area. Eq. (22), (23), (24) yield the components of the cumulative reaction force which according to Newton's third law have to be equal to the components of the applied load. Finally, Eq. (25) gives the expression for the cumulative frictional torque.

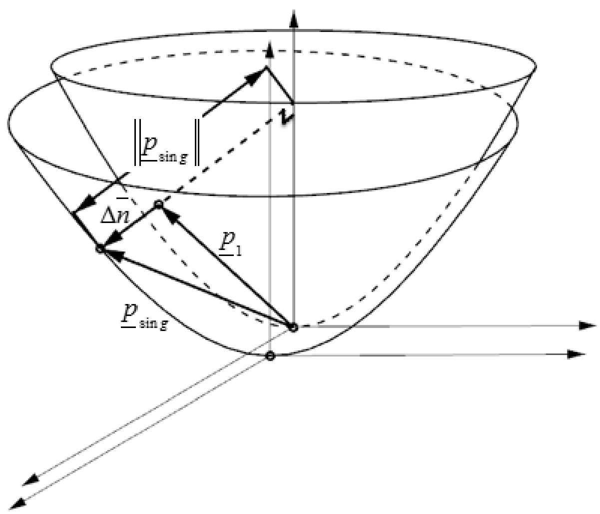

Figure 10. Representation of moment arm

4. APPLICATION TO SOME COMMON SURFACE GEOMETRIES:

4.1. Concentric spherical annulus:

Consider two concentric spherical surfaces (Figure 12) created by the revolution of:

$$z_1 = f_1(r_1) = \sqrt{R_1^2 - r_1^2} \Rightarrow z_1' = \frac{-r_1}{\sqrt{R_1^2 - r_1^2}} \tag{26}$$

$$z_2 = f_2(r_2) = \sqrt{R_2^2 - r_2^2} \Rightarrow z_2' = \frac{-r_2}{\sqrt{R_2^2 - r_2^2}} \tag{27}$$

with:

$$\underline{F} = \begin{bmatrix} 0 & 0 & F^{sph} \end{bmatrix} \tag{28}$$

$$\underline{e} = \begin{bmatrix} 0 & 0 & \varepsilon \end{bmatrix} (\varepsilon < 0) \tag{29}$$

$$R_2 \approx R_1 - \varepsilon \ \ (|\varepsilon| << R_1, R_2) \tag{30}$$

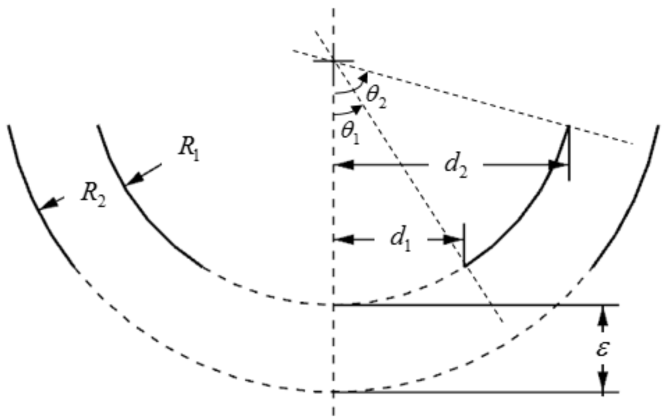

Figure 11. Schematic of a concentric spherical annulus

Dropping the subscript of r_1, φ_1. It can be readily verified that $\Delta(r, \varphi) = -\varepsilon$ and:

$$\overline{n_1} = \overline{n_2} = \begin{bmatrix} \dfrac{-r}{R_1}\cos(\varphi) & \dfrac{-r}{R_1}\sin(\varphi) & \dfrac{\sqrt{R_1^2 - r^2}}{R_1} \end{bmatrix}^T \tag{31}$$

Thus from Eq. (16) and Eq. (18):

$$\Im(r, \varphi) = \delta + \varepsilon \tag{32}$$

$$\underline{p'}_{\sin g} = \begin{bmatrix} \left(1 - \dfrac{\varepsilon}{R_1}\right) r\cos(\varphi) & \left(1 - \dfrac{\varepsilon}{R_1}\right) r\sin(\varphi) & 0 \end{bmatrix}^T \tag{33}$$

$$\left\| \tilde{p}'_{\sin g} \underline{n}_f \right\| \approx \left\| \underline{p'}_{\sin g} \right\| = \left(1 - \frac{\varepsilon}{R_1}\right) r \tag{34}$$

Substitute Eq. (1), (26), (32), (34) into Eq. (25), we attain the frictional torque expression:

$$\left\|\underline{T}_f^{sph}\right\| = \frac{4}{3}\mu E^* \Re_o^{1/2} \aleph_0 R_2 \times I_\delta I_r I_\varphi \tag{35}$$

where:

$$I_\varphi = \int_0^{2\pi} d\varphi = 2\pi$$

$$I_\delta = \int_{\Delta=\varepsilon}^{\infty} (\delta+\varepsilon)^{3/2} \frac{1}{\sqrt{2\pi}R_q} \exp\left(-\frac{\delta^2}{2R_q^2}\right) d\delta$$ (I_δ can be solved using Eq. (2))

$$I_r = \int_{d_1}^{d_2} \frac{r^2}{\sqrt{R_1^2 - r^2}} dr = \frac{1}{2}\left(R_1^2 \arctan\left(\frac{r}{\sqrt{R_1^2 - r^2}}\right) - r\sqrt{R_1^2 - r^2}\right)\Bigg|_{d_1}^{d_2}$$

4.2. Eccentric cylindrical annulus:

Consider two cylindrical surfaces (Figure 13) defined by the revolution:

$$r_1 = R_1 \Rightarrow z_1' = \infty \tag{36}$$

$$r_2 = R_2 \Rightarrow z_2' = \infty \tag{37}$$

with:

$$\underline{F} = \left[F^{cyl}\cos(\varphi_1) \quad F^{cyl}\sin(\varphi_1) \quad 0\right] \tag{38}$$

$$\underline{e} = \left[\varepsilon\cos(\varphi_1) \quad \varepsilon\sin(\varphi_1) \quad 0\right] \tag{39}$$

$$dA = hR_1 d\varphi_1 \tag{40}$$

Eq. (15) then becomes:

$$\begin{Bmatrix} \varepsilon + R_2\cos(\varphi_2) \\ R_2\sin(\varphi_2) \\ h_2 \end{Bmatrix} = \begin{Bmatrix} \Delta(R_1,\varphi_1)\cos(\varphi_1) + R_1\cos(\varphi_1) \\ \Delta(R_1,\varphi_1)\sin(\varphi_1) + R_1\sin(\varphi_1) \\ h_1 \end{Bmatrix} \begin{matrix} (a) \\ (b) \\ (c) \end{matrix}$$

Squaring (a) and (b) then take their sum:

$$R_2^2 = (\Delta.\cos(\varphi_1) + R_1 \cos\varphi_1 - \varepsilon)^2 + (\Delta.\sin(\varphi_1) + R_1 \sin\varphi_1)^2$$
$$\Leftrightarrow R_2^2 = \Delta^2 + 2\Delta R_1 - 2\Delta\varepsilon\cos(\varphi_1) + R_1^2 - 2\varepsilon R_1 \cos(\varphi_1) + \varepsilon^2$$
$$\Leftrightarrow \Delta^2 + [2R_1 - 2\varepsilon\cos(\varphi_1)]\Delta + [R_1^2 - R_2^2 - 2\varepsilon R_1 \cos(\varphi_1) + \varepsilon^2$$

After solving for Δ and dropping higher order terms of ε, we get:

$$\Delta \approx R_2 - R_1 + \varepsilon\cos(\varphi_1) \tag{41}$$

Solve for $\cos(\varphi_2), \sin(\varphi_2)$ then substitute into Eq. (12) and Eq. (13):

$$\overline{n_1} = \begin{bmatrix}\cos(\varphi_1) & \sin(\varphi_1) & 0\end{bmatrix}^T \tag{42}$$

$$\overline{n_2} = \Bigg[\cos(\varphi_1) - \frac{\varepsilon}{R_2}\sin^2(\varphi_1) \quad \sin(\varphi_1) + \frac{\varepsilon}{R_2}\cos(\varphi_1)\sin(\varphi_1) \tag{43}$$

$$\Rightarrow \overline{n_1}^T\overline{n_2} = 1$$

Thus from Eq. (16), (18) and (19):

$$\Im(r_1, \varphi_1) = \delta - \Delta = \delta - (R_2 - R_1 + \varepsilon\cos(\varphi_1)) \tag{44}$$

$$\underline{p'}_{\sin g} = \begin{bmatrix}(R_1 + \Delta)\cos(\varphi_1) & (R_1 + \Delta)\sin(\varphi_1) & 0\end{bmatrix}^T \tag{45}$$

$$\left\|\tilde{p}'_{\sin g}\, \underline{n}_f\right\| \approx \big(2(R_2^2 \sin^2(\varphi_1)\cos^2(\varphi_1) + 2\varepsilon\sin^2(\varphi_1)\cos^3(\varphi_1) \tag{46}$$

Substitute Eq. (1), (35), (44), (46) into Eq. (21), (22), (25), we attain the contact area, applied load and cumulative frictional torque expressions:

$$A^{cyl} = \pi\Re_0\aleph_0 \frac{1}{\sqrt{2\pi}R_q} R_1 h \times \int_0^{2\pi}\int_\Delta^\infty \exp\left(-\frac{\delta^2}{2R_q^2}\right)(\delta - (R_2 - R_1 + \tag{47}$$

$$F_x^{cyl} = \frac{4}{3} E^* \Re_o^{1/2} \aleph_0 \frac{1}{\sqrt{2\pi} R_q} R_1 h$$
$$\times \left[\int_0^{2\pi} \int_\Delta^\infty \exp\left(-\frac{\delta^2}{2R_q^2} \right) (\delta - (R_2 - R_1 + \varepsilon \cos(\varphi_1)))^{3/2} \ (\cos(\right. \tag{48}$$

$$\left\| \underline{T}_f^{cyl} \right\| = \frac{4}{3} \mu E^* \Re_o^{1/2} \aleph_0 \frac{1}{\sqrt{2\pi} R_q} R_1 h$$
$$\times \left[\int_0^{2\pi} \int_\Delta^\infty \exp\left(-\frac{\delta^2}{2R_q^2} \right) (\delta - (R_2 - R_1 + \varepsilon \cos(\varphi_1)))^{3/2} \right. \tag{49}$$
$$\times \left(2R_2^2 \sin^2(\varphi_1) \cos^2(\varphi_1) + 2\varepsilon \left(3\sin^2(\varphi_1) \cos^3(\varphi_1) - \mathrm{s} \right. \right.$$

5. ANALYSIS:

However, the eccentricity ($\underline{e}$) is hard to measure without special instruments. Thus it is more convenient to consider the frictional torque – load relationship. By eliminating $\underline{e}$ using Eq. (22) to Eq. (25), we can find:

$$\left\| \underline{T}_f \right\| = \tau(\underline{F}, \mu, R_q, G_i) \tag{50}$$

where:

$\underline{F}$ and μ are the applied load and the friction coefficient

R_q is RMS roughness parameter

G_i 's are the surfaces geometric parameters

$$\left\| \underline{T}_f^* \right\| = \tau'(G_i) \mu \left\| \underline{F} \right\| \tag{50}$$

Which means the frictional torque is linearly dependent on the applied load value. It is expected that $\left\| \underline{T}_f^* \right\| \approx \left\| \underline{T}_f \right\|$ and the two values become closer if more assumptions about the geometries are made. For example, in Section IV.1, if we assume $R_2 \approx R_1 - \varepsilon \ \left(|\varepsilon| << R_1, R_2 \right)$, then from Eq.(24) and Eq. (25):

$$A^{cyl} = \pi\Re_0\aleph_0 \frac{1}{\sqrt{2\pi}R_q} R_1 h \times \int_0^{2\pi}\int_{\Delta}^{\infty} \exp\left(-\frac{\delta^2}{2R_q^2}\right)(\delta - (R_2 - R_1 + \tag{52}$$

After replacing $d_1 = R_1\sin(\theta_1)$, $d_2 = R_1\sin(\theta_2)$, Eq. (50) becomes:

$$A^{cyl} = \pi\Re_0\aleph_0 \frac{1}{\sqrt{2\pi}R_q} R_1 h \times \int_0^{2\pi}\int_{\Delta}^{\infty} \exp\left(-\frac{\delta^2}{2R_q^2}\right)(\delta - (R_2 - R_1 + \tag{53}$$

Eq. (53) is exactly the formula for the frictional torque – applied load relationship if the contacting surfaces are modeled as smooth that is obtained in several studies such as the one from Grégory (2014).

Considering the example in Section 4.2 where no additional geometric assumption is made. First, the consistency between theories of contact mechanics should be taken into account. In the early days, Hertz set the foundation of contact mechanics by analytically predicting the compressive force required to indent a smooth sphere into a infinite smooth half-space, which was then broadened to account for other shapes. According to Sneddon 1965, in the case of parallel-axis cylinders contact, the applied force as function of indentation depth $\varepsilon + R_1 - R_2$ is:

$$F_{smooth} = \pi h(\varepsilon + R_1 - R_2)/4 \tag{54}$$

Thus Eq. (48) should be identical to Eq. (54) as $R_q = 0$ since both describe contact in the "smooth" case. Taking the limit of Eq. (48):

$$\begin{aligned} F_{rough}(0) &= \lim_{R_q\to 0} F_x^{cyl} = \frac{4}{3}E^*\Re_o^{1/2}\aleph_0 R_1 h \\ &\times \lim_{R_q\to 0}\left[\int_0^{2\pi}\int_{\Delta}^{\infty}\frac{1}{\sqrt{2\pi}R_q}\exp\left(-\frac{\delta^2}{2R_q^2}\right)(\delta-(R_2-R_1+\varepsilon\cos(\varphi_1)))^{3/2}\,(\cos(\varphi_1)-\frac{\varepsilon}{R_2}\sin^2(\varphi_1))d\delta d\varphi_1\right] \end{aligned} \tag{55}$$

Noting that the Gaussian distribution function becomes the Dirac delta function as $R_q \to 0$, which has a special property:

$$\int \delta_\alpha f(x) = f(0) \tag{55}$$

Using this property, Eq. (54) becomes:

$$F_{rough}(0) = \frac{4}{3} E^{*} \Re_{o}^{1/2} \aleph_0 R_1 h \times \int_0^{2\pi} (R_1 - R_2 - \varepsilon \cos(\varphi_1))^{3/2} (\cos(\varphi_1) - \frac{\varepsilon}{R_2} \sin^2(\varphi_1)) d\delta d\varphi$$

Let

$$I_{\varphi_1} = \int_0^{2\pi} (R_1 - R_2 - \varepsilon \cos(\varphi_1))^{3/2} (\cos(\varphi_1) - \frac{\varepsilon}{R_2} \sin^2(\varphi_1)) d\delta d\varphi$$

The analytical solution for this definite integral could be found using Wolfram Alpha:

$$\begin{aligned} I_{\varphi_1} = \frac{2\sqrt{a+b}}{105 b^2} \Bigg\{ & \left(6a^3c - 21a^2b + 58ab^2c - 63b^3\right) \left[E\left(2\pi \middle| \frac{2b}{a+b}\right) - E\left(0 \middle| \frac{2b}{a+b}\right) \right] \\ & - (a-b)\left(6a^2c - 21ab + 10b^2c\right) \left[F\left(2\pi \middle| \frac{2b}{a+b}\right) - F\left(0 \middle| \frac{2b}{a+b}\right) \right] \Bigg\} \end{aligned} \tag{56}$$

where:

$a = R_2 - R_1, \quad b = \varepsilon, \quad c = \varepsilon / R_2$

$F(\cdot)$ and $E(\cdot)$ are the incomplete elliptic integrals of first and second kind

Since it is required that $F_{rough}(0) = F_{smooth}$, we attain:

$$\frac{4}{3} E^{*} \Re_{o}^{1/2} \aleph_0 R_1 h = \frac{\pi h(\varepsilon + R_1 - R_2)}{4I} \tag{57}$$

Next, using Eq. (2), (3) we could analytically evaluate the first integrations in Eq. (47), (48), (49). Based on these expressions, a MATLAB script is written to numerically evaluate Eq. (47), (48) and (49) at increments of ε and R_q. The integration command "integral" uses global adaptive quadrature method "integral" with absolute error tolerance of 1e-10 (Shampine, 2008).

Graphs 1 to Graph 6 show the relationships between contact area, applied force, frictional torque with eccentricity and roughness. Graph 7 indicates that even though the contact area – applied load relationship might be linear at a particular roughness, the contact area increases faster with applied load as roughness goes up. We even observe this behavior more clearly in the case of frictional torque – applied load relationship.

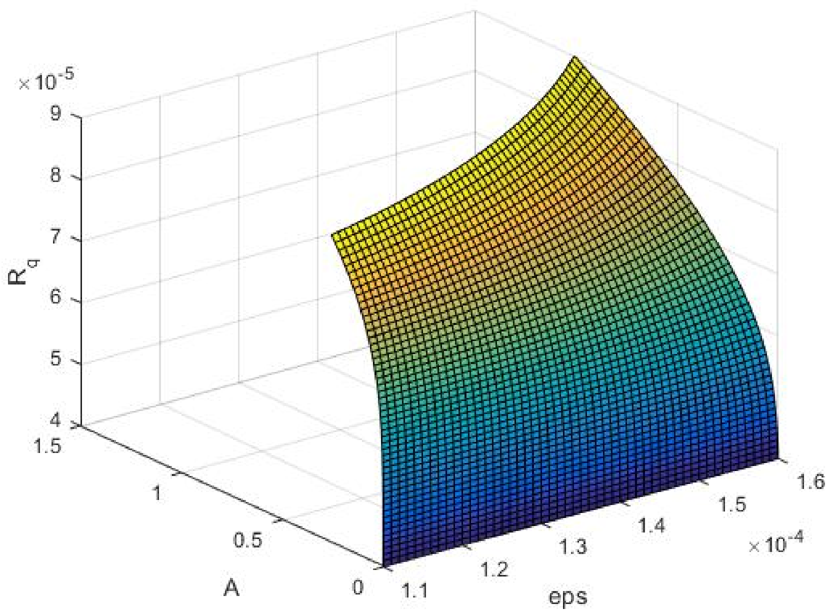

Graph 1. Contact area as function of eccentricity and roughness

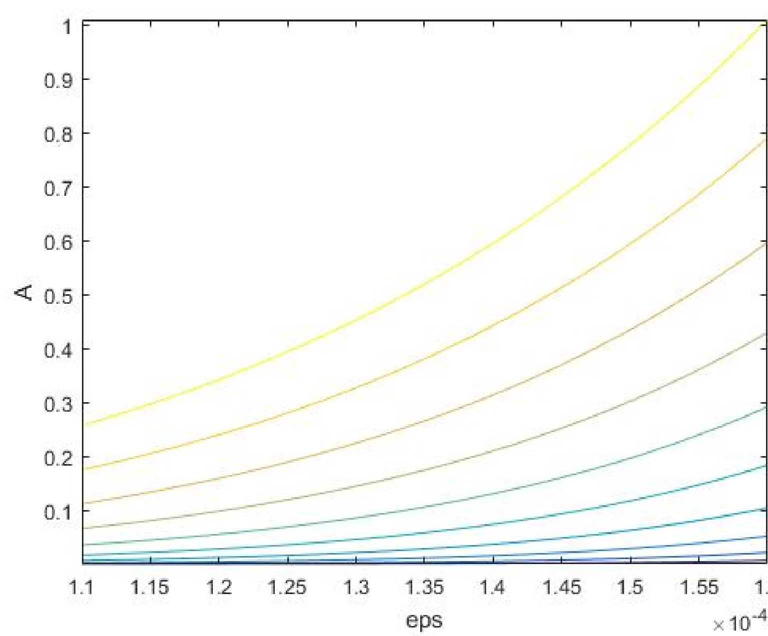

Graph 2. Contact area as function of eccentricity at various roughness

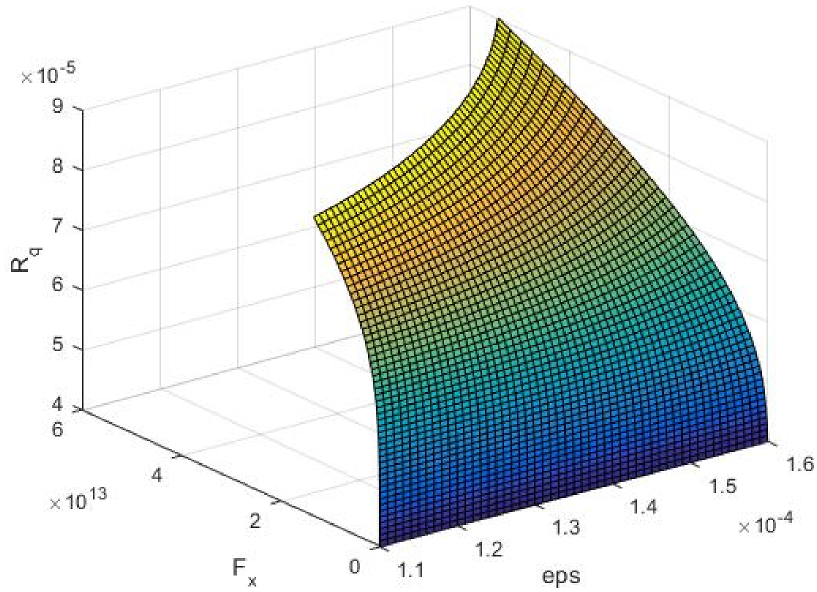

Graph 3. Applied force as function of eccentricity and roughness

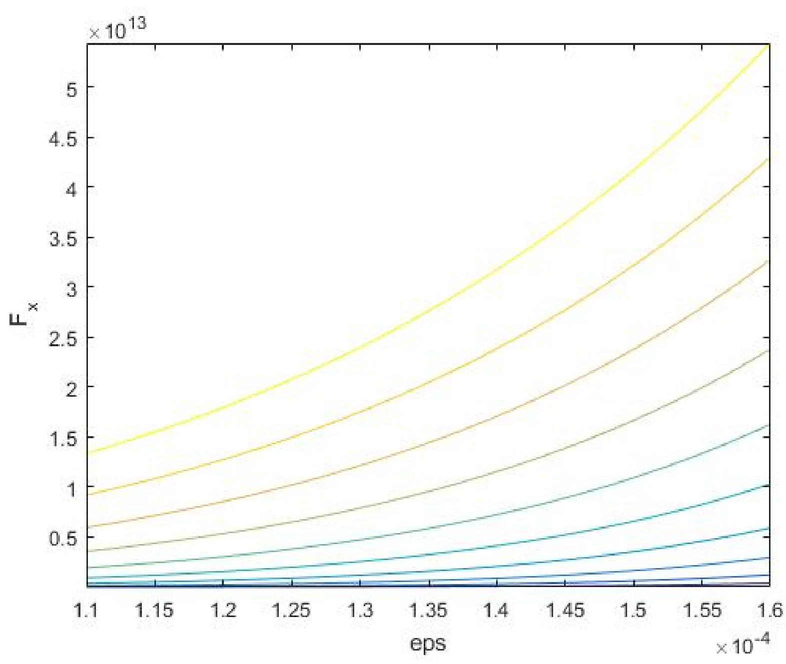

Graph 4. Applied force as function of eccentricity at various roughness

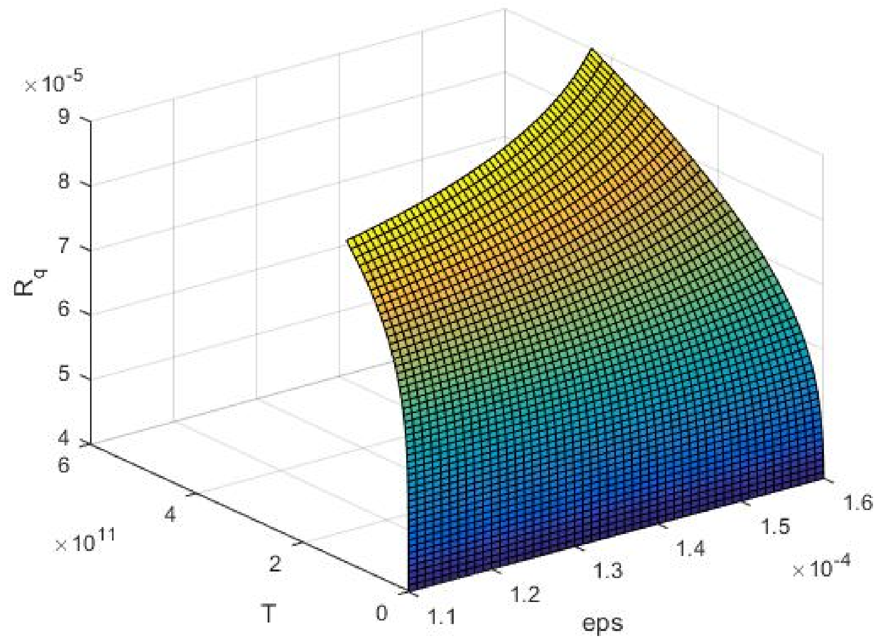

Graph 5. Frictional torque as function of eccentricity and roughness

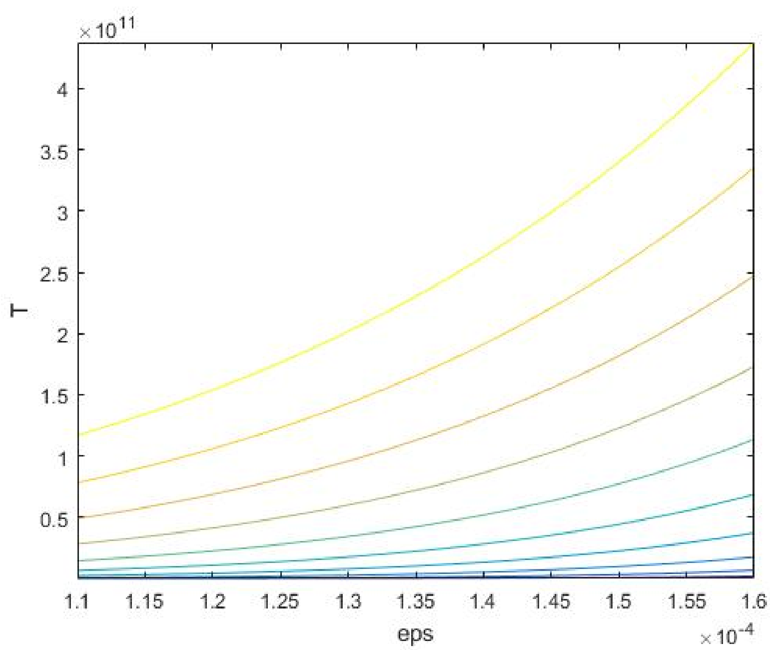

Graph 6. Frictional torque as function of eccentricity at various roughness

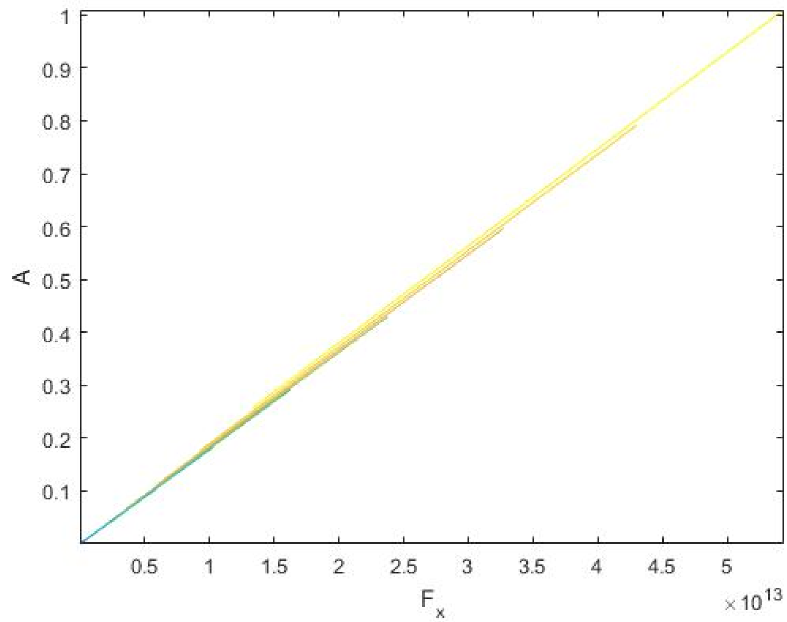

Graph 7. Contact area as function of applied force at various roughness

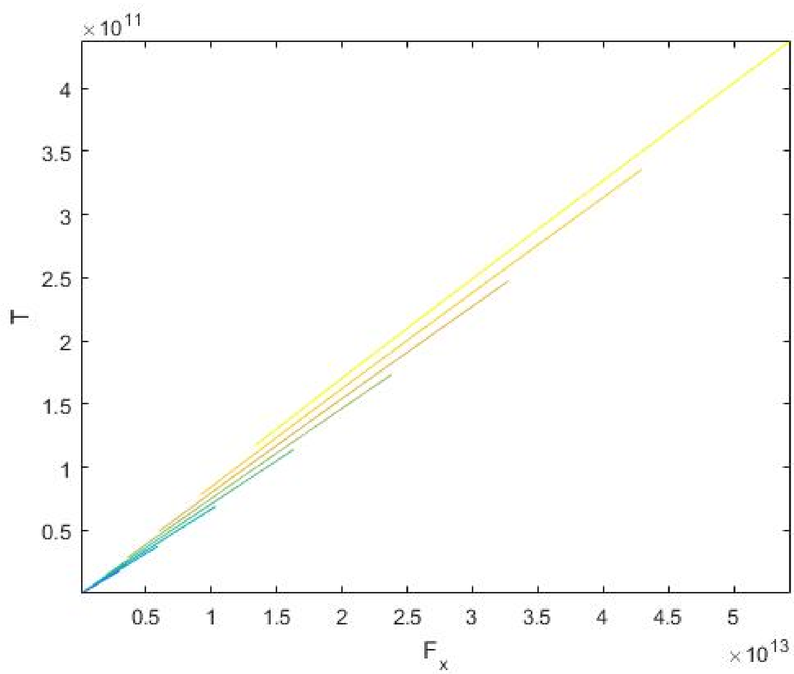

Graph 8.Frictional torque as function of applied force at various roughness

6. CONCLUSION

The paper proposes a method to account for the contact of rough curved surface having nearly identical geometries. General formulas for the true contact area as well as the applied force have been deduced in terms of definite integrals. These integrals could be simplified analytically. Numerical technique and programming are then implemented in order to perform analysis of a special case: two cylindrical rough surfaces in contact.

REFERENCES

[1] Anton, H., 1999, Calculus: A New Horizon, sixth ed., Wiley, New York.

[2] Bhushan, B., 2001, Surface Roughness Analysis and Measurement Techniques, in: Bhushan, B. (Ed.), Modern Tribology Handbook, CRC Press, Boca Raton.

[3] Blau, P.J., 2001, The significance and use of friction coefficient, Tribology International, 34(9), 585-591.

[4] Gray, A., 1997, Surfaces of Revolution, Modern Differential Geometry of Curves and Surfaces with Mathematica, second ed., Boca Raton, CRC Press, Florida, 457-480.

[5] Greenwood, J.A., Williamson, J.B.P. (1966) Contact of nominally flat surfaces, Proceedings of the Royal Society A, 295(1442), 300–319.

[6] Grégory, A., 2014, On the Mechanical Friction Losses Occurring In Automotive Differential Gearboxes, The Scientific World Journal, 2014.

[7] Jackson, R.L., et al., 2013, Contact mechanics, in: Menezes, P.L., Nosonovsky, S., Lovell, S., (Eds.), Tribology for Scientists and Engineers, Springer, New York.

[8] Jackson, R. L., Green, I., 2011, On the Modeling of Elastic Contact between Rough Surface, Tribology Transactions, 54, 300-314.

[9] Liu, S.B., 2005, An extension of the Hertz theory for three-dimensional coated bodies, Tribology Letters, 18(3), 303–314.

[10] Lu, W., 2014, Prediction of Surface Topography at the End of Sliding Running-In Wear Based on Areal Surface Parameters, Tribology Transactions, 57(3), 553-560.

[11] Menezes, P.L., et al., 2013, Fundamentals of Engineering Surfaces, in: Menezes, P.L., Nosonovsky, S., Lovell, S., (Eds.), Tribology for Scienties and Engineer, Springer, New York.

[12] MuPAD, Symbolic Math in MATLAB, https://www.mathworks.com/discovery/mupad.html

[13] Shampine, L.F., 2008, MATLAB Program for Quadrature in 2D, Applied Mathematics and Computation, 202(1), 266–274.

[14] Sneddon, I. N., 1965, The Relation between Load and Penetration in the Axisymmetric Boussinesq Problem for a Punch of Arbitrary Profile, International Journal of Engineering Science, 3(1), 47-57.

[15] Yastrebov, V.A., Anciaux, G., Molinari, J.F., From Infinitesimal to Full Contact between Rough Surfaces: Evolution of the Contact Area, International Journal of Solids and Structures, 52, 83-102.